



UNIVERSITÀ POLITECNICA DELLE MARCHE  
Repository ISTITUZIONALE

Dynamic monitoring of buildings as a diagnostic tool during construction phases

This is the peer reviewed version of the following article:

*Original*

Dynamic monitoring of buildings as a diagnostic tool during construction phases / Nicoletti, V.; Arezzo, D.; Carbonari, S.; Gara, F.. - In: JOURNAL OF BUILDING ENGINEERING. - ISSN 2352-7102. - ELETTRONICO. - 46:(2022). [10.1016/j.jobe.2021.103764]

*Availability:*

This version is available at: 11566/293681 since: 2024-05-30T11:26:09Z

*Publisher:*

*Published*

DOI:10.1016/j.jobe.2021.103764

*Terms of use:*

The terms and conditions for the reuse of this version of the manuscript are specified in the publishing policy. The use of copyrighted works requires the consent of the rights' holder (author or publisher). Works made available under a Creative Commons license or a Publisher's custom-made license can be used according to the terms and conditions contained therein. See editor's website for further information and terms and conditions.

This item was downloaded from IRIS Università Politecnica delle Marche (<https://iris.univpm.it>). When citing, please refer to the published version.

(Article begins on next page)

# Dynamic monitoring of buildings as a diagnostic tool during construction phases

Vanni Nicoletti<sup>a1</sup>, Davide Arezzo<sup>a</sup>, Sandro Carbonari<sup>a</sup>, Fabrizio Gara<sup>a</sup>

<sup>a</sup> Dept. ICEA, Università Politecnica delle Marche, Via Brecce Bianche, 60131 Ancona, Italy.

## Abstract

The paper discusses the usefulness of the dynamic characterization of buildings based on the use of ambient vibration tests at different construction phases. The proposed experimental procedure, integrated with more conventional non-destructive in-situ tests for the estimation of the material mechanical properties, foresees the monitoring of the evolution of the building modal properties during the main construction phases. The monitoring makes it possible to assess the correctness of the construction through comparison with expected trends, and to consider possible countermeasures in case of unexpected behaviours. A case study, monitored during its construction, is presented to show the additional value of information obtained from the proposed experimental approach: (i) tests on the bare frame can be adopted to validate the design numerical model of the structure, in which non-structural elements are neglected in performing ultimate limit state verifications, (ii) the proposed monitoring allows the identification of the infills contribution on the building dynamics, providing useful information to address the interaction problem between structural and non-structural elements that may be detrimental at ultimates, and (iii) trends of resonance frequencies during the construction, validated through numerical applications, constitute an important tool for interpreting data from structural health monitoring system, as well as to establish alert thresholds of demand parameters (e.g. relevant to the building occupancy or structural damage).

*Keywords:* building construction phases, dynamic monitoring, modal parameters evolution, ambient vibration tests, non-destructive in-situ tests, infilled RC frame building, dynamic proof test, structural health monitoring.

## 1. Introduction

From a technical point of view, the final certificate of construction of a building is usually released at the end of the construction before the structure can be used by the owner. The inspector certify that the construction respects the building regulations and that the structure complies with the designed one. However, for important constructions (i.e. requiring particular construction processes, or constructions that are not fully inspectable after their completion) an inspector is appointed at the beginning of the works with the aim of controlling all the construction phases, including technical aspects, which have to comply with the design drawings, and quality aspects.

The construction process of a building can be monitored with the aim of controlling that both structural and non-structural components are built following the design drawings, as well as the adopted

---

<sup>1</sup> Corresponding author: Department of Civil and Building Engineering, and Architecture, DICEA, Università Politecnica delle Marche, Via Brecce Bianche, 60131 Ancona, Italy - E-mail address: v.nicoletti@pm.univpm.it

construction materials and techniques comply with the design prescriptions. This monitoring, although not always mandatory, is very useful and can be adopted as a support for the editing of the final certificate; indeed, identifying and correcting structural problems during construction is easier and cheaper than at the end. When mandatory, the monitoring is usually done through periodic surveys on the building site and visual inspections, in order to verify if the typology and geometry of the structural and non-structural elements are correct. However, also Non-Destructive in-situ Tests (NDTs) can be performed to control some features of the structure or the mechanical properties of the construction materials.

Among NDTs, this paper analyses the usefulness of using Ambient Vibration Tests (AVTs) to characterise the building dynamics during its construction. Indeed, AVTs lead to identify the modal properties of the building at each construction stage, permitting the identification of possible structural anomalies through the comparison of data with the expected ones, obtained from the numerical structural model. Both modelling and realization mistakes may be detected, relating for example to the restraints and the values and distribution of the masses in the modelling, as well as to the dimensions of structural members and the material stiffness. In addition, for Reinforced Concrete (RC) structures, tests can be performed in absence of infills, which are built at the end of the frames, making it possible to experimentally identify the modal properties of the bare frame through which the complete design numerical model can be validated. AVTs present the advantage to be easy and fast to perform and requires the positioning of sensors (and eventually cables) that do not interfere with the construction procedures, making their execution possible without interrupting the construction works (by obviously considering all the necessary safety measures).

The idea of using AVTs during the construction of a building to progressively validate the construction stages is quite original. Most of the studies available in the literature are based on vibration data collected from completed structures; it is the case of [1-5], where AVTs are adopted to investigate the dynamic behaviour of tall buildings during their life, or [6-11], where vibration data are collected on low- and medium-rise buildings. Some researchers try to use vibration measurements to investigate the infill contribution on the building dynamics, but again, in most cases, the measurements were performed in completed buildings [12-15] or after the non-structural components damage [16-17]. Only few works deal with the dynamic investigation of buildings during construction. As an example, in [18] ambient response measurements were made on an 18-storey building at three different stages of construction to detect any changes in the frequencies, mode shapes and stiffness during the construction process. In [19] the results of a study on the variability of the dynamic properties of an irregular high-rise building during its construction are illustrated, while in [20] a Structural Health Monitoring (SHM) network was installed during the construction of a 56-storey building to record the ambient excitation during the construction

for over two-year period, permitting to identify the building dynamic behaviour that was used to validate the construction process and the computer design model. Finally, some works deal with the system identification of real-scale specimens that are tested in different phases during the construction procedures: in [21] and [22] the construction phases of the structure and the non-structural components are widely investigated, both through ambient excitation and induced vibrations. Also, in [23] a full-scale specimen is tested during different construction phases, even if the main aim of the work is to investigate the evolution of the modal parameters due to a progressively induced damage.

In addition to AVTs, other common NDTs can be performed in order to control the RC building construction correctness. It is the case of Penetration Tests (PTs) and Rebound Hammer Tests (RHTs), which furnish an indication of the concrete compressive strength of the structural members already built, or of the Ultrasonic Pulse Tests (UPTs), which provide an indication of the concrete quality and its uniformity within the whole building. In addition, UPTs lead to obtain an estimation of the dynamic elastic modulus of concrete, which can be compared with the static one, generally calculated based on code formulas and estimated through compressive tests on concrete samples. Also, Pull Out Tests (POTs) are commonly performed on existing buildings to estimate the concrete compressive strength, but they are discouraged in case of new buildings since they foresee a test protocol that produce a little damage to the tested member. In addition to these common tests, other unconventional NDTs can be performed, especially in case of structures with great relevance or that require complicated construction techniques. As an example, radioactive methods can be also adopted, along with X-Ray Tests (XRTs), which permit the investigation of the interior of a RC structural member, i.e. the presence and amount of rebars, stirrups, steel cables (in prestressed concrete), concrete defects and cracks. Obviously, being this test typology potentially dangerous for the human health, it must be used when necessary and with all the required cautions. An alternative NDT that provides an estimation of the perimetric rebar amount and size is the Covermeter Test (CT).

The paper proposes a simple, fast and cheap strategy to assess the construction correctness of RC buildings based on the monitoring of the modal properties during construction, and the comparison of the experimental evolution with the expected one. The procedure is based on the use of AVTs for the dynamic characterisation of the global structure, integrated with more conventional NDTs, for the estimation of the material mechanical local properties, and the use of Impact Load Tests (ILTs), through which the In-Plane (IP) stiffness of infills can be estimated, adopting the procedures proposed in [24]. NDTs and ILTs are fundamental to calibrate the building numerical model that must provide the benchmark for the control of the evolution of the modal parameters, especially in terms of resonance frequencies, and that can be used for the SHM of the building during its life.

## 2 The proposed strategy for monitoring buildings during construction phases

The proposed strategy to control the building construction stages (i.e. their consistency with the design requirements) is based on the use of AVTs on the whole building, ILTs on infill walls, and conventional NDTs on RC structural members to estimate the material mechanical properties. For RC structures, the latter integrates the standard destructive laboratory tests on steel rebars and concrete cube specimens performed for material acceptance issues.

AVTs allow the characterization of the dynamic behaviour of the building expressed in terms of modal parameters, namely resonance frequencies, damping ratios and mode shapes, furnishing information about the global behaviour of the building related to mass and stiffness distribution. The tests can be performed during the main construction phases, obtaining the evolution of the building modal parameters during the time consistently with the building evolution, from the beginning to the end of the construction. In particular, these tests can be performed in key stages of the construction process and, with reference to RC frame structures, they can be executed after each deck casting, as well as at the end of the construction of the bare frame structure, i.e. before the non-structural elements (e.g. external and internal infills) are added. Tests on the bare frame are of particular interest because the identified modal parameters can be suitably adopted to validate the design numerical model of the structure, in which non-structural elements are commonly neglected for verifications at ultimate limit states. By observing the evolution of modal parameters and by comparing the experimental results with the expected trend, the latter predicted exploiting the numerical model adopted for the design, it can be verified in a simple and direct way if the building construction is correctly evolving. Any anomalous trend in the dynamic behaviour can be immediately detected and may trigger the decision-making process for carrying out investigations to search causes of the anomalies.

By assuming that the nature of the first resonance frequency does not change during the construction (i.e. it is always representative, for example, of the translational vibration mode), Figure 1 shows a typical time-frequency evolution for the first vibration mode of an infilled RC frame building during construction. This curve can be built by tracing the frequency value of the considered vibration mode during different construction phases, represented with grey triangles in Figure 1, and in key phases of the construction, represented with dark grey circles. Independently on the numerical predictions, some peculiar aspects of the expected trend can be herein discussed. In detail, if key point A represents, for example, the construction of the first storey of a multi-storey building (columns, beams and deck), and key point B the completion of the bare frame, the frequency shows a clear decreasing trend from A to B both for the addition of masses and for the reduction of the overall stiffness of the building, due to the increased height.

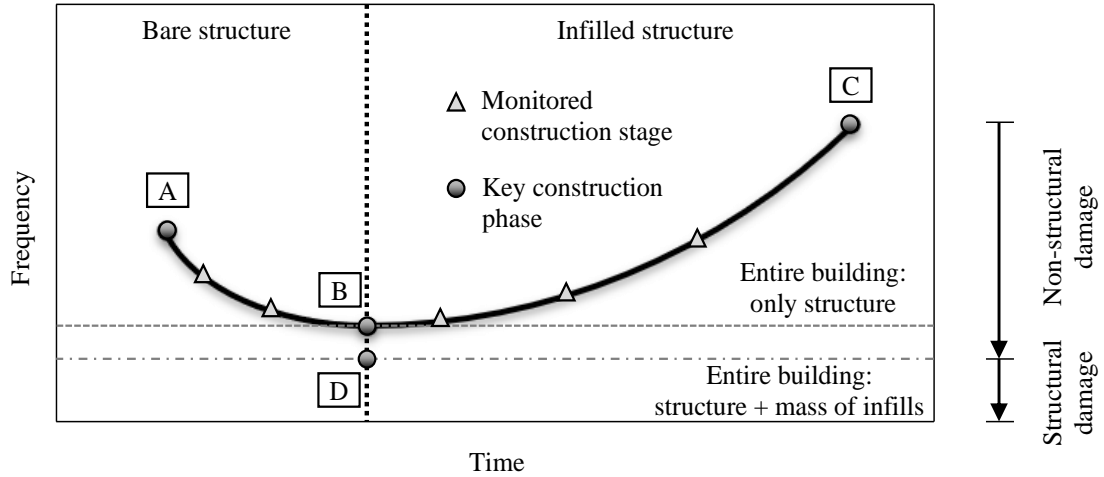


Figure 1. Typical frequency evolution during construction phases for low- and medium-rise infilled RC frame buildings.

Moreover, this decreasing trend is more evident (high slope) in the first part of the curve, and gradually becomes less important approaching key point B, because the increase in mass and the decrease in stiffness becomes progressively lower as compared with the total mass and stiffness of the portion of the building already built. Furthermore, for RC frames, the first mode shape is typically characterized by high interstorey drifts at the lower floors and low interstorey drifts at the higher ones, meaning that by increasing the building height the mass increase is more important than the floor stiffness; this contributes to the above discussed typical trend of the curve. Contrarily, if key point C represents the building at the end of construction, from B to C the frequency shows a clear increasing trend; this demonstrates that the non-structural components (especially infills) have a great effect on the overall stiffness of the building, producing a frequency increase greater than the decrease due to the increment of the total mass. In view of the great contribution to the stiffness given by the infill walls, it is worth noting that the proposed monitoring strategy foresees the identification of the infills contribution on the building dynamics, which is a very timely and investigated aspect in recent years [24-27]. It is worth mentioning that the frequency evolution proposed in Figure 1 is representative for low- and medium-rise infilled RC frame buildings and the trend may differ for high-rise buildings [28], for which the mass increasing due to the addition of infills has great effects on the building dynamic behaviour, reducing the increasing trend of frequency between key points B and C. Finally, key point D of Figure 1 represents the building in which only the mass of the infills is considered, neglecting the stiffness. For this reason, the relative frequency value can be evaluated only by numerical predictions, adopting a numerical model that is very similar to that commonly adopted during the design process in the professional practice.

The experimental evolution of the resonance frequencies (the main resonance frequencies can be considered) can be compared with the predicted one obtained from the numerical model. In this

framework, up to key point B, the numerical predictions are quite easy since the overall numerical model developed for the design, which usually excludes the contribution of non-structural components in terms of stiffness, has only to be modified by eliminating the masses of the non-structural elements, e.g. infill walls and pavement. Starting from key point B up to C, the need of including the stiffening contribution of infills, together with their mass, occurs. This can be done by adding, consistently with the construction phase that is monitored, infills to the numerical model through the use of shell elements. The material elastic modulus to be used for the infill wall modelling can be easily experimentally estimated according to the procedure proposed by Nicoletti et al. [24]. This methodology consists in performing ILTs on selected infills in order to identify their Out Of Plane (OOP) dynamic behaviour, expressed in terms of natural frequencies and mode shapes. Then, the infills are included as homogeneous, isotropic, elastic thin plates within a numerical model of the building, and a calibration procedure is performed according to a proposed algorithm.

Once the resonance frequency trends are available and validated through comparisons with numerical data, they can be suitably used as an important tool for the building monitoring during its life, and for the interpretation of data from SHM system, if installed on the building. First of all, key point C in Figure 1 represents the situation of the building at the end of the construction, and thus a benchmark frequency value that, if matched in future dynamic measurements resulting nearly constant with time, probably confirms the absence of any damage on the structure. In this sense, it should be remarked that identified resonance frequencies of real buildings through AVTs presents a dependency with the ambient parameters (such as temperature and wind) and the interpretation of data should account for these issues [29-31]. Besides, a frequency value identified between key points C and D may indicate a possible damage occurred to non-structural elements, being D the frequency evaluated numerically by considering the contribution of non-structural members only in terms of masses. Finally, with high probability, an identified frequency below key point D may reveal a structural damage.

The proposed monitoring strategy and the relevant benchmark curves in terms of frequency evolution in time, may be of particular interest in the case of strategic building (such as hospitals, schools, fire and police stations), for which also the integrity of non-structural components is an important issue to consider in order to guarantee the building occupancy after exceptional events for the emergency management.

The proposed approach of monitoring can take advantage of classical NDTs, such as UPTs and RHTs. They allow the investigation of the concrete mechanical properties, including its homogeneity throughout the structure, and they can be used as an important support that integrates the compressive tests on cubic specimens, which are commonly executed for new buildings for material acceptance issues. Indeed, destructive tests are performed on suitable specimens that are casted during the

construction and may be not fully representative of the in-situ concrete. Furthermore, these tests have to be performed, at least, twenty-eight days after the casting, so the results may be available after a period of time that is often not compatible with the timing of the construction site. Besides, UPTs and RHTs allow an estimate of the concrete compressive strength by correlating results of destructive tests with those obtained from each test separately, or with those obtained by jointly elaborating results of the two tests according to the well-known SONREB [32] methodology. Data obtained from above tests can be suitably implemented in the numerical model that has to provide the predictions of the frequency evolution.

### **3 Application of the proposed monitoring strategy to a real strategic building during the construction phases**

The application of the proposed monitoring strategy to a real case study is shown in this Section. The considered building is a newly built fire station located in the Marche Region, in central Italy (Figure 2). The building has 58.50 x 14.80 m rectangular plan and total height of 15.65 m (with three storeys above the ground level and a basement). The structure is constituted by RC frames and RC precast floor slabs with polystyrene blocks for the first two storeys and hollow tiles mixed floors for the last two storeys (Figure 2d). The foundation system consists of 20 m deep drilled piles with caps connected by tie beams in transverse and longitudinal directions. The concrete grade for the superstructure (C28/35) is higher with respect to that of the foundations (C25/30) and the design concrete mechanical properties are reported in Table 1. The building presents two RC stairs, each one developing around an elevator that is supported by a steel structure disconnected from the RC frame. Part of the roof is constituted by sandwich panels supported by a steel structure; these flank a central corridor that connects two lateral pavilions characterised by a flat roof. The basement is bordered around by a 0.30 m thick retaining RC wall and a RC pile bulkhead, both located 0.9 m away from the frame and connected to the main building only at the foundation level; thus, there is no interaction between the retaining structures and the frame, and the gap at the ground level is covered by means of cantilever RC slabs or steel grids. All the internal and external infill masonry walls are made with the hollow clay bricks reported in Figure 2e. Double brick walls are sometimes used for the external perimeter to improve insulation; External walls (E) and Internal walls (I) can be both divided into three typologies, as shown in Figure 2f. Hereafter, labels E# and I# will be used to indicate the different wall typologies. E1 is used to build all the external infill masonry walls at the underground level; E2 is used for the external walls of the two pavilions located at the edges of the building, starting from the ground level up to the last elevation. E3 is used for the external walls of the East and West building façades from the ground up to the last floor.



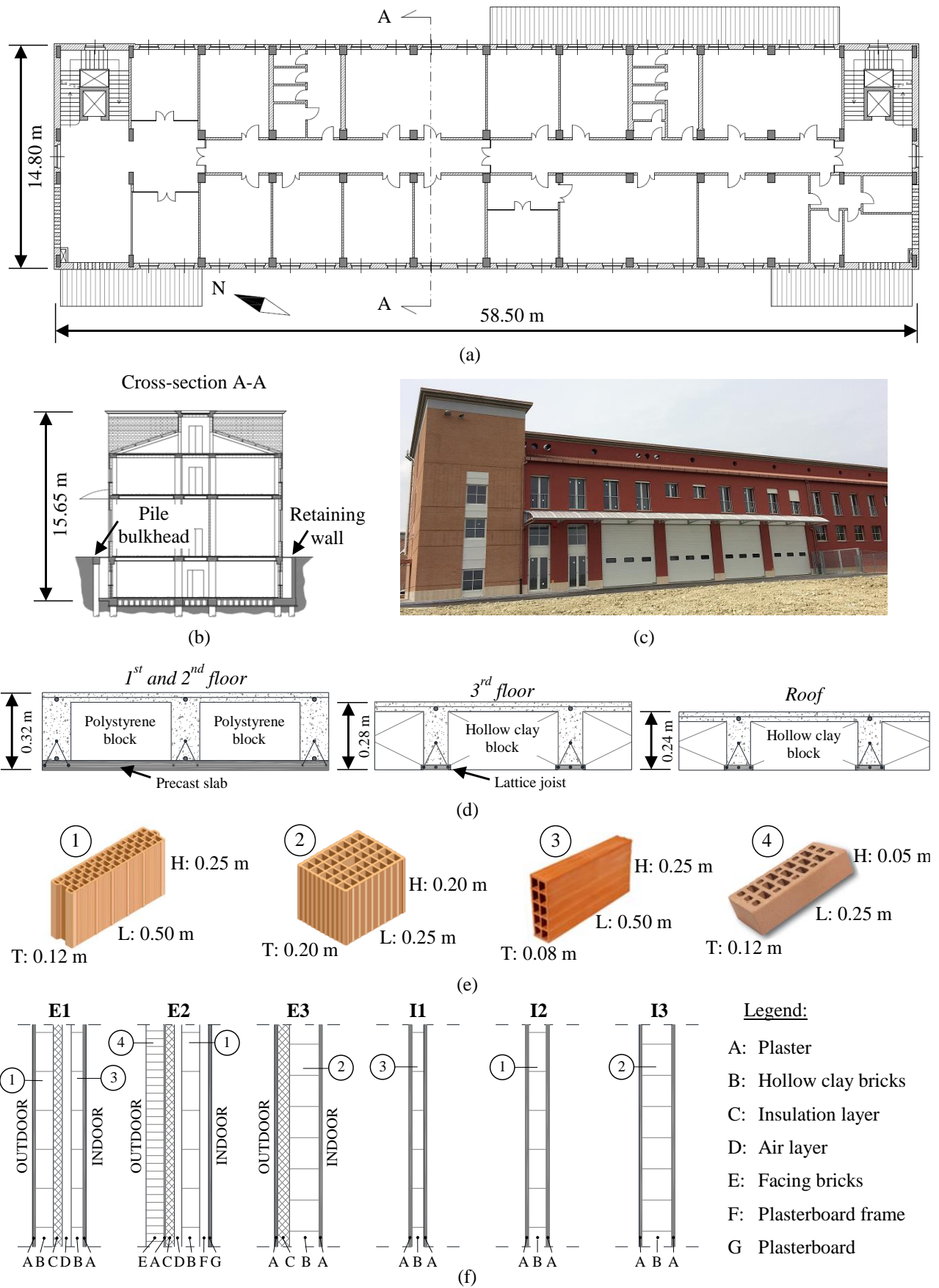


Figure 2. Building case study: (a) plan of the 2<sup>nd</sup> floor, (b) transverse cross-section, (c) external view, (d) floor slab typologies, (e) bricks adopted for external and internal infills, (f) external and internal infill typologies.

Table 1. Design values of concrete mechanical properties.

| Property   | Foundations | Superstructure |
|--|-------------|----------------|
| Characteristic cubical compressive strength $R_{ck}$ [MPa]     | 30          | 35             |
| Characteristic cylindrical compressive strength $f_{ck}$ [MPa] | 25          | 28             |
| Elastic modulus $E_c$ (Static) [GPa]                           | 31.4        | 32.5           |

It is worth mentioning that the external infill masonry walls relevant to the East and West façades are longer than those on the North and South façades and are characterised by wider openings. Considering interior walls, I1 is used for most of the internal infills at the first floor while I2 is adopted for most of internal walls at the underground and ground floors, as well as for the internal panels of the staircases at each elevation. Finally, I3 is used to separate garages from offices both at the underground and ground floors, and for some of the external infill masonry walls of the two lateral pavilions at the last floor.

The building was monitored in key stages during its construction, which began in May 2016; the entire monitoring includes many phases that can be subdivided into two main groups: the first relevant to the construction of the bare RC frame (B) and the second to the construction of the infill walls (I), constituting the main non-structural elements of the building. As concerns the bare structure construction, four phases are considered: July 11<sup>th</sup> (B1), when the foundation system, the 1<sup>st</sup> and 2<sup>nd</sup> elevation columns and stairs, and the 1<sup>st</sup> floor were completely constructed; July 29<sup>th</sup> (B2), when the 2<sup>nd</sup> floor and the 3<sup>rd</sup> elevation columns and stairs were built; August 22<sup>nd</sup> (B3), when the 3<sup>rd</sup> floor and the 4<sup>th</sup> elevation columns and stairs were constructed; and August 25<sup>th</sup> (B4), at the end of the bare structure construction (after the roof concrete casting). Considering the infill construction process, three phases are taken into account: September 12<sup>th</sup> (I1), when the basement and the ground floor infills were built; September 26<sup>th</sup> (I2), when the 1<sup>st</sup> floor infills were completed; and November 7<sup>th</sup> (I3), at the end of the attic floor infill construction. Finally, the last construction phase corresponds to the building completion and refers to April 6<sup>th</sup> (I4), 2017, when all the non-structural components and devices were installed, including the two elevators. All the monitoring phases are schematized in Figure 3, while Figure 4 shows some pictures relevant to the building construction.

### 3.1 Ambient vibration tests on the building

AVTs are performed at key stages of the construction process to identify the global dynamic behaviour of the building during its construction and to track the evolution of its modal parameters. A total of eight AVTs are performed, corresponding to the eight investigated phases: the first four relating to the construction of the bare frame structure, the following three to the construction of the infill walls, and the last one to the complete building ready for the use.

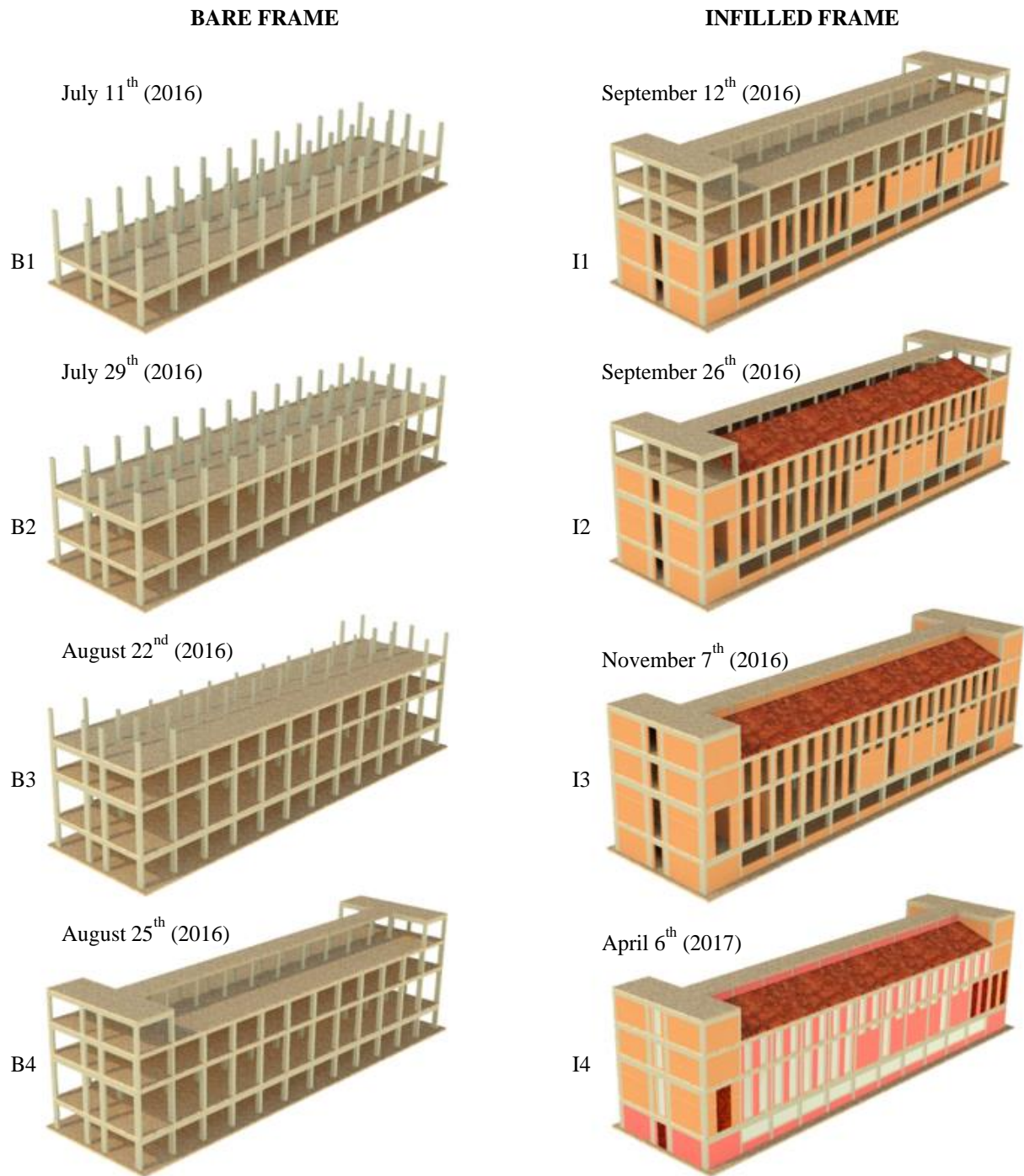


Figure 3. Building construction process with the eight main phases considered for the monitoring.



Figure 4. Pictures relevant to the construction process of the building.



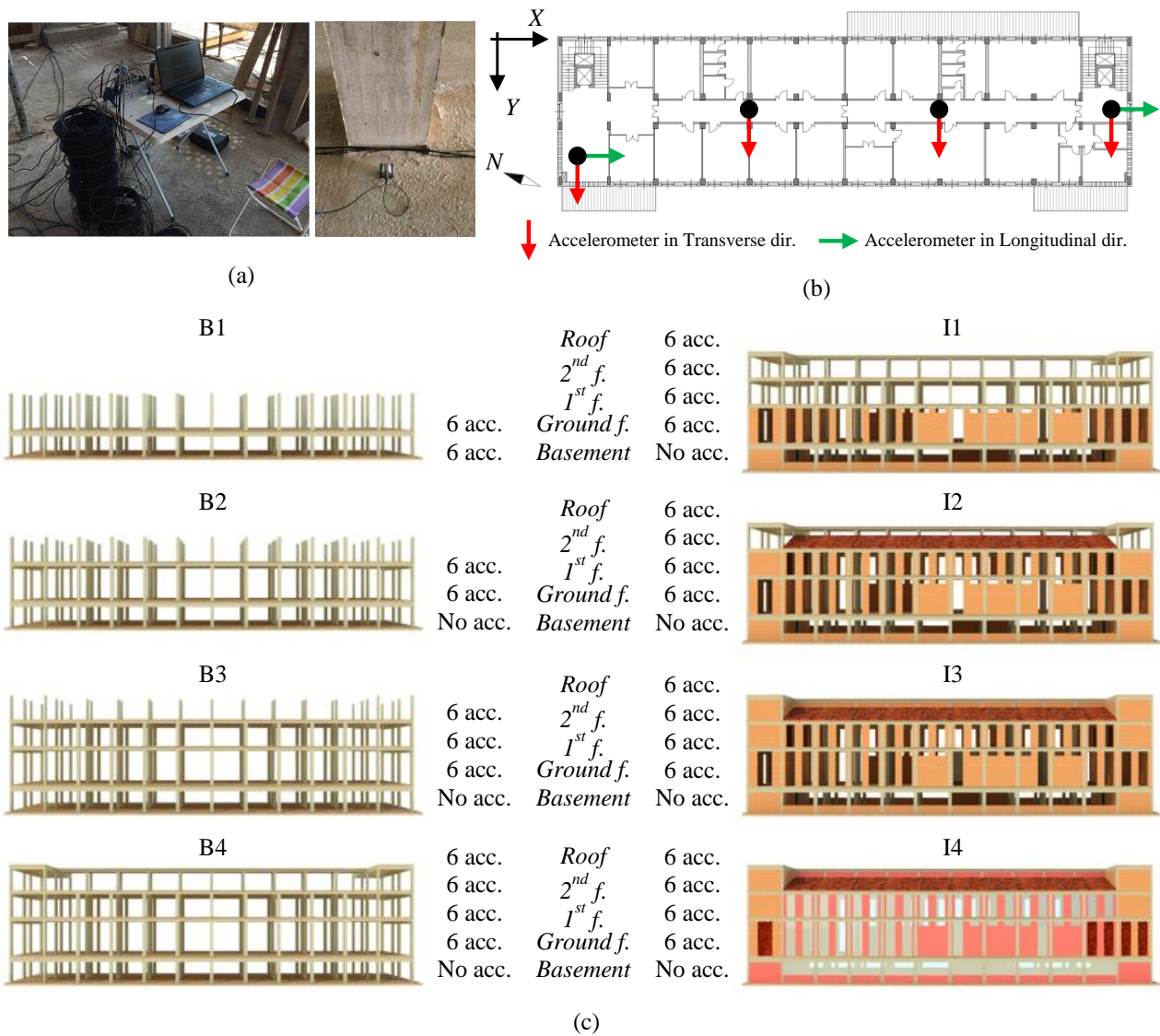


Figure 5. AVTs during construction: (a) pictures of the adopted instrumentation, (b) layout of sensors at a generic floor, (c) sensors employed at different construction stages.

For the dynamic tests at each monitoring phase, the instrumentation (Figure 5a) consisted in low-noise uniaxial piezoelectric accelerometers PCB model 393B31 (sensitivity of 10 V/g, frequency range of 0.07 – 300 Hz, and 1  $\mu$ g of resolution), connected by means of coaxial cables to a 4-channels dynamic signal acquisition module NI-9234 mounted on a USB chassis NI cDAQ9178, and a notebook equipped with a dedicated software for data storage and real-time tracking of the recorded time histories. For each test, at least half-an-hour-long acceleration time histories were recorded with a sampling frequency of 2048 Hz. As an example, in Figure 6a the time histories of the accelerations recorded from the sensor placed at the North-West corner of the building at the roof floor, are reported; in details, records during B4 and I4 construction phases are shown in order to make comparisons between the excitation level inherent to the bare frame and the complete building.

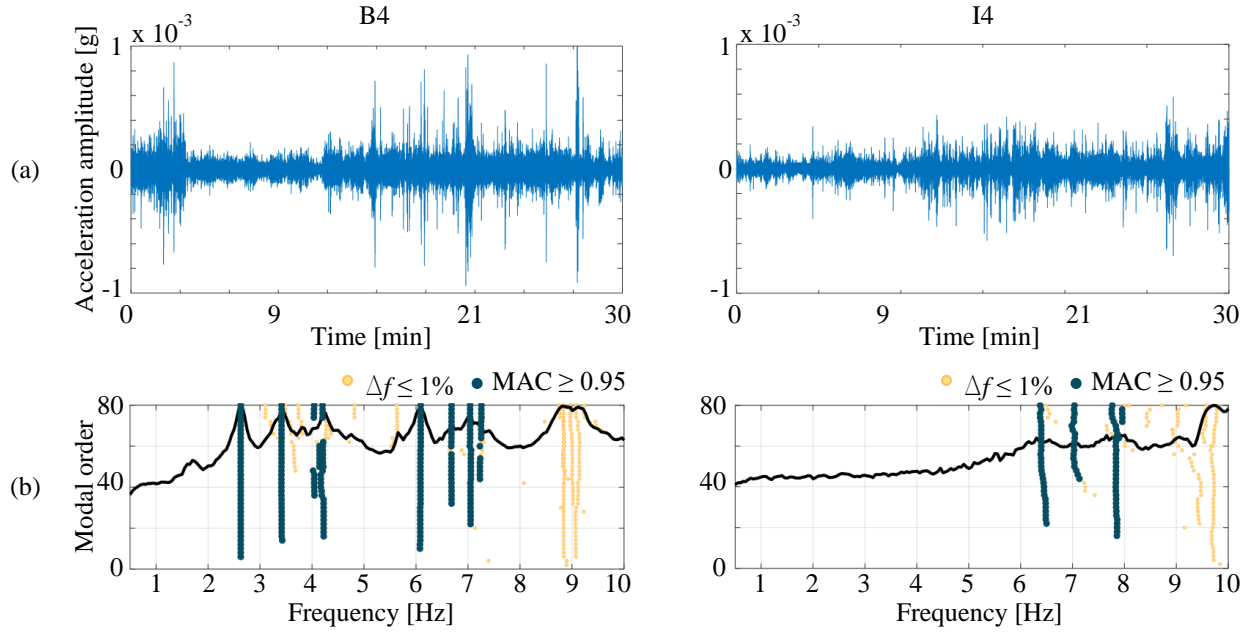


Figure 6. AVT records and results relevant to the bare frame (B4) and the complete building (I4): (a) time histories of the accelerations at the roof floor, (b) stabilization diagrams.

For the investigated building, the ambient excitation was mainly due to microtremors, wind, construction activities, and traffic, being the building built in proximity of a busy road.

Sensors were positioned over the floors according to the layout shown in Figure 5b, which is the same for all elevations, from the basement to the roof. Usually, for RC framed buildings with compact plan shape, the IP rigid floor assumption is realistic and hence only three accelerometers per floor are necessary to identify the dynamic behaviour and to plot the first mode shapes of the building with good accuracy. In this case, six sensors per floor instead of three were adopted in order to also investigate possible IP floor deflections triggered by the slender rectangular plan shape, and to obtain more detailed building mode shapes. For the first dynamic test (B1) sensors were positioned at the basement and at the ground floor levels, whereas for the subsequent tests, sensors were positioned only from the ground floor level to the building top, neglecting those at the basement because of the low level of excitations found. For tests requiring a high number of sensors (more than the available), AVTs were performed adopting different configurations and the results are obtained by merging data from the different tests on the basis of reference sensors that are common to all the acquisitions, according to well-established methodologies available in the literature. In detail, mode shapes are obtained through post processing procedures that exploit the Post Separate Estimation Re-scaling (PoSER) methodology [33]. A resume of the sensor layout for all the monitoring phases is reported in Figure 5c.

The experimental modal parameters are identified through Operational Modal Analyses (OMAs) starting from the recorded vibration measurements. The Covariance-driven Stochastic Subspace Identification (SSI-COV) [34] output-only technique is adopted to this purpose. A self-made Matlab

routine based on this technique is implemented, in order to identify the modal parameters starting from AVT measurements and adopting a stabilization diagram as a support. As an example, Figure 6b shows the stabilization diagrams obtained from tests B4 and I4; the stable modes in terms of frequency (difference less than 1%) and mode shape (MAC greater than 0.95) are identified by a yellow and a dark blue solid circle, respectively. The first singular value obtained from the singular value decomposition performed on the cross power spectral density matrix, represented with a black line, is also reported. This shows clear peaks for the bare frame in correspondence of the vibration mode resonance frequencies while for the complete building the peaks are less evident; however, the identification method is efficient in finding stable modes in all the cases.

### *3.2 Evolution of the experimental modal properties during construction*

The modal parameters of the building are identified from the eight performed AVTs and monitored to evaluate the effects of the main construction activities. In particular, the first three vibration modes are identified at each phase and their evolution in time is traced.

As for frequency values, Figure 7a and Table 2 report their variations from the beginning to the end of construction. As expected, the trend of frequencies complies with the general one described in Figure 1. From B1 to B4, during the first four phases relevant to the bare frame construction, the resonance frequencies decrease, because of the mass increment due to added stories (floors and concrete members) and of the overall stiffness decrement due to the increase of the building height. Furthermore, the variation reduces approaching B4, because the increase in mass and the decrease in stiffness becomes progressively lower as compared with the total mass and stiffness of the portion of the building already built. The effect of formwork and shoring is almost negligible, since they do not contribute to the building lateral stiffness and their masses can be considered very small with respect to the building total mass.

Then, from B4 to I4, all natural frequency values increase, mainly due to the lateral stiffening contribution provided by the infills, which is predominant with respect to the effect of their masses. A less important contribution can be instead attributed to the increase of the concrete elastic modulus during the curing process [35]. In detail, observing curves from B4 to I3 (when all infills were built), it is possible to note that the frequency of the first vibration mode doubles, passing from 2.62 Hz to 5.34 Hz, the second frequency is 70% higher, passing from 3.40 Hz to 5.89 Hz, and the third is 60% higher, with values shifting from 4.19 Hz to 6.70 Hz. Results confirm the important role of infill masonry walls on the building lateral stiffness. Comparing the frequencies between I3 and I4 (when the building was completed), a further frequency increase is noticeable (around 13% for the first, 9% for the second and 5% for the third mode, respectively), demonstrating that also non-structural components and devices

mounted on the building (such as cladding, plasters, system installations, elevators, etc.) increase the lateral stiffness of the structure; indeed, the increase of the concrete Young's modulus with time, which rapidly reduces after the first month, is not sufficient to justify this frequency increment.

Focusing on damping ratios, also in this case the values reported in Figure 7b and Table 3 show a trend that can be associated to the different construction stages. Indeed, the damping ratios for the first three vibration modes are nearly constant from B1 to B4, ranging around 1.35% to 2.99%, which are typical values for bare RC frame structures subjected to ambient excitations; in reality, a slight decrease is observed with the increase in the number of stories, which could be due to a lower percentage contribution from the soil-foundation interaction, which is characterized by greater damping compared to the RC structure [36]. After that, the values of damping ratios start to gradually increase, probably due to the kinematic interaction between the non-structural components and the frame structure. Those corresponding to I3 are around 5-6%, which are typical values for RC buildings, as also suggested by codes. The highest values around 6-7% are registered on I4, demonstrating that the non-structural component and devices can also influence the damping ratio estimated through OMA from AVTs.

Figure 8 depicts the evolution of the first three mode shapes and the relevant Complexity Plots (CPs). As can be seen, during the entire construction process, the first mode corresponds to the first longitudinal mode (in X-direction), the second mode to the first transverse mode (in Y-direction) and the third mode to the rotational one. The mode shapes of the transverse modes in Y-direction are always characterised by an IP floor deformation, which exhibits higher modal displacements at mid-length of the floors and lower displacements at the ends. An indication of the mode complexity is provided by the CPs associated to each mode shape, together with the relevant Modal Complexity Factor (MCF), the latter calculated as the ratio between the area of the polygon drawn around the extremities of the individual vectors and the area of the circle drawn based on the length of the largest vector element. The MCFs are lower for tests around the complete bare frame, while they are higher at the beginning and when the infills are progressively built, getting maximum values for the complete building. A further comparison between mode shapes is reported in Figure 7c and in Table 4 in terms of Modal Assurance Criterion (MAC) indexes [37]. This index indicates how two mode shapes are similar to each other: the closer the index to one, the greater the likeness between mode shapes. The comparison is made for each vibration mode and between two subsequent tests (i.e. the 1<sup>st</sup> vs 1<sup>st</sup>, the 2<sup>nd</sup> vs 2<sup>nd</sup> and the 3<sup>rd</sup> vs 3<sup>rd</sup>). As can be observed the comparison leads to high MAC values, always greater than 0.75 and, often, greater than 0.90 (excluding the MACs between I4 and I3), attesting that the mode shapes remain roughly the same during the construction, validating consistency of the previous comparisons in terms of natural frequencies and damping ratios, which implicitly assumed that the modes evolved maintaining their order. Only from I3 to I4 there is a greater mode shape variation (especially for the first and third modes

that have MAC values of 0.74 and 0.69, respectively); however, the vibration mode classification remains the same, as can be noted by observing Figure 8. Finally, a more comprehensive comparison between all the mode shapes is reported in Figure 9 where each mode shape, at each construction phase, is compared with all the others. The calculated MAC are reported graphically in a matrix using a grey scale plot: black colour corresponds to MAC values equal to one, while white colour to MAC values equal to zero. The diagonal entries represent the comparison between a mode and itself; consequently, they assume MAC index equal to one (black box). Three almost black big areas are evident in the matrix, which still confirms that the  $i$ -th vibration mode shape remains almost the same for all the construction phases.

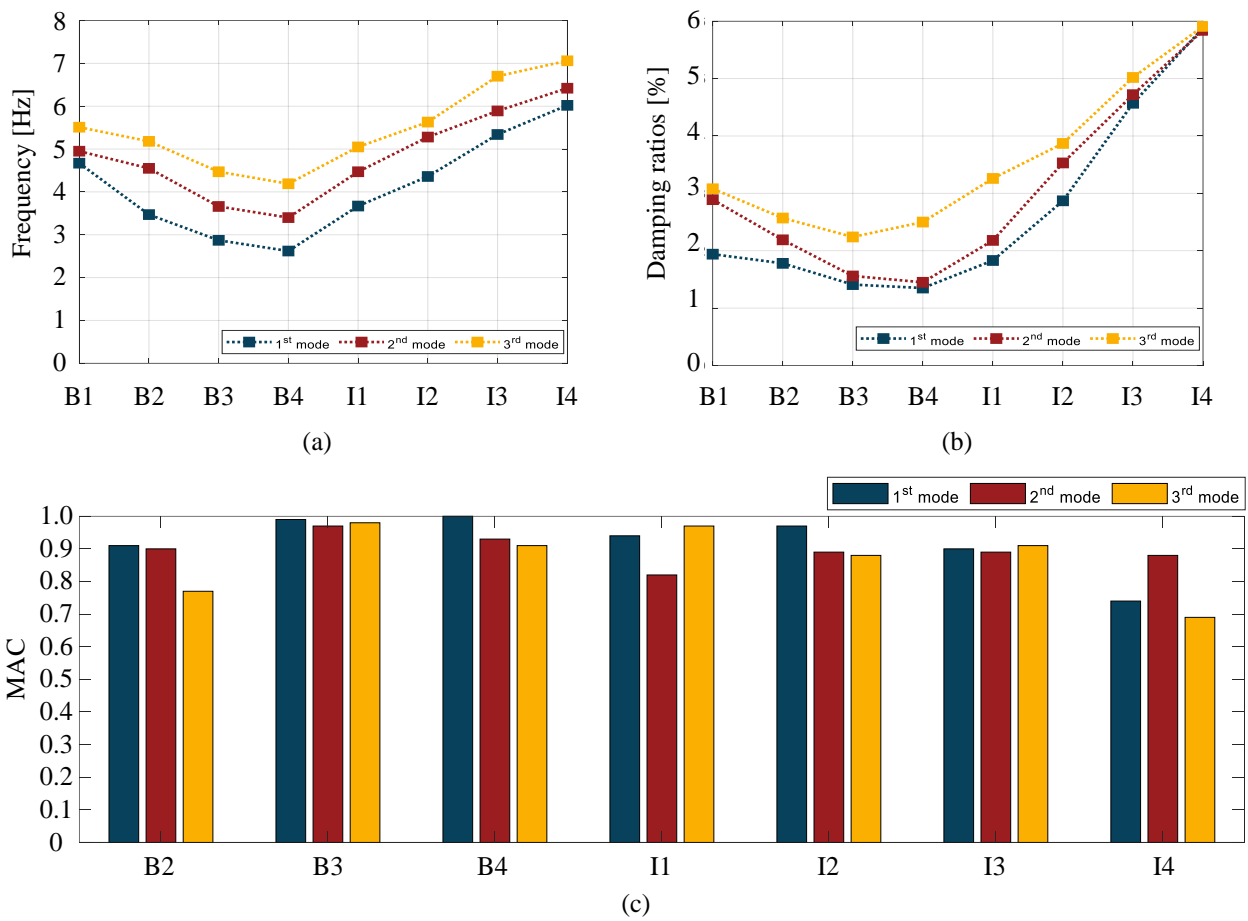


Figure 7. Evolution of the building modal parameters during construction: (a) resonance frequencies, (b) damping ratios, (c) MAC values.

Table 2. Building resonance frequencies during construction.

| Mode                 | Frequency [Hz] |      |      |      |      |      |      |      |
|----------------------|----------------|------|------|------|------|------|------|------|
|                      | B1             | B2   | B3   | B4   | I1   | I2   | I3   | I4   |
| 1 <sup>st</sup> mode | 4.67           | 3.47 | 2.87 | 2.62 | 3.67 | 4.36 | 5.34 | 6.02 |
| 2 <sup>nd</sup> mode | 4.95           | 4.55 | 3.66 | 3.40 | 4.47 | 5.28 | 5.89 | 6.42 |
| 3 <sup>rd</sup> mode | 5.51           | 5.18 | 4.47 | 4.19 | 5.05 | 5.63 | 6.70 | 7.06 |



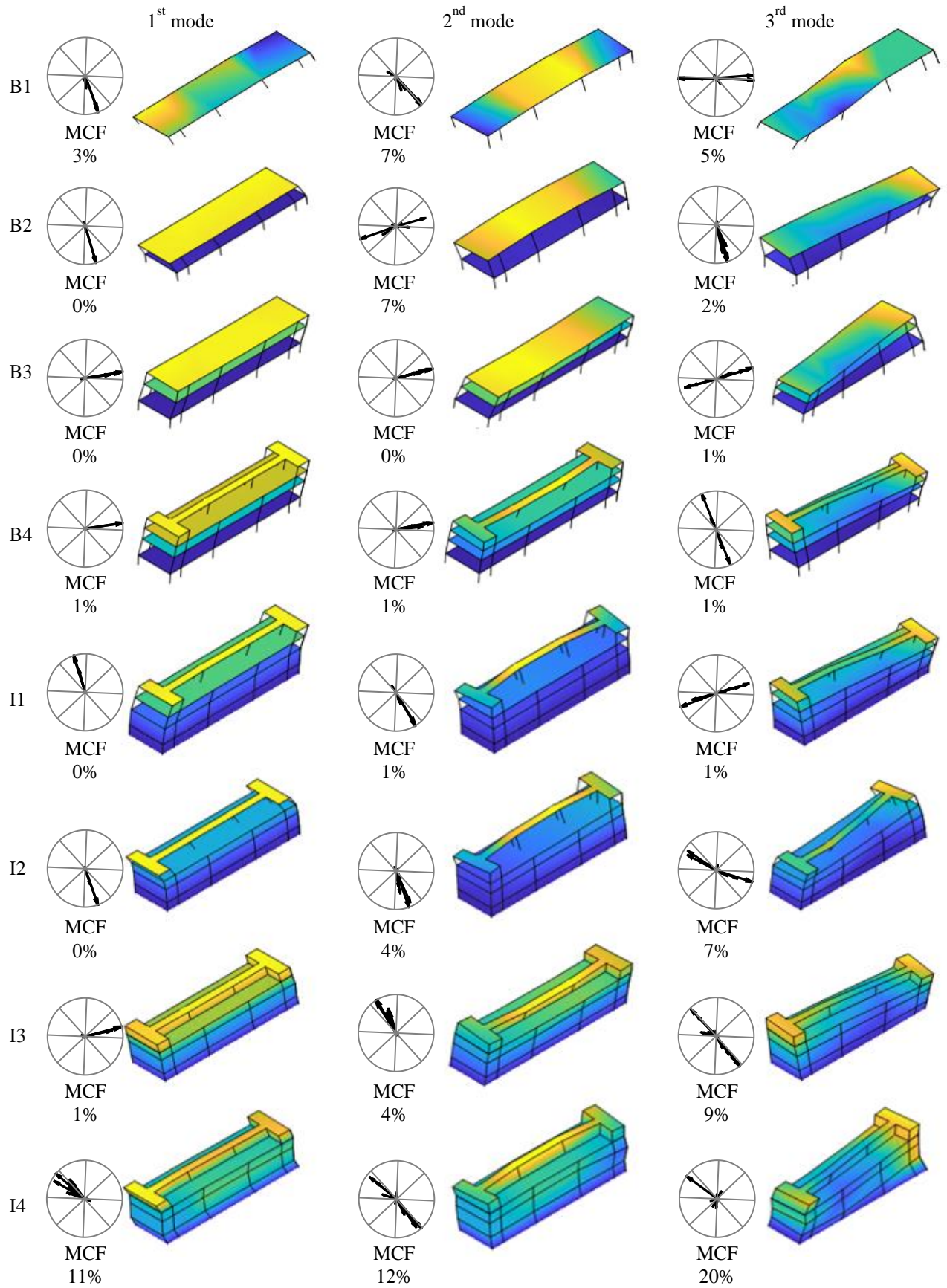


Figure 8. Evolution of the first three building mode shapes and the relevant CPs and MCFs during construction.

Table 3. Building damping ratios during construction.

| Mode                 | Damping ratio [%] |      |      |      |      |      |      |      |
|----------------------|-------------------|------|------|------|------|------|------|------|
|                      | B1                | B2   | B3   | B4   | I1   | I2   | I3   | I4   |
| 1 <sup>st</sup> mode | 1.80              | 2.03 | 2.06 | 1.35 | 1.83 | 2.87 | 4.57 | 5.88 |
| 2 <sup>nd</sup> mode | 2.89              | 2.19 | 1.56 | 1.45 | 2.18 | 3.53 | 4.72 | 5.84 |
| 3 <sup>rd</sup> mode | 2.99              | 2.57 | 2.24 | 2.71 | 3.26 | 3.87 | 5.02 | 5.91 |

Table 4. MAC values of the first three building mode shapes during construction.

| Mode                 | MAC      |          |          |          |          |          |          |
|----------------------|----------|----------|----------|----------|----------|----------|----------|
|                      | B2 vs B1 | B3 vs B2 | B4 vs B3 | I1 vs B4 | I2 vs I1 | I3 vs I2 | I4 vs I3 |
| 1 <sup>st</sup> mode | 0.91     | 0.99     | 1.00     | 0.94     | 0.97     | 0.90     | 0.74     |
| 2 <sup>nd</sup> mode | 0.90     | 0.97     | 0.93     | 0.82     | 0.89     | 0.89     | 0.88     |
| 3 <sup>rd</sup> mode | 0.77     | 0.98     | 0.91     | 0.97     | 0.88     | 0.91     | 0.69     |

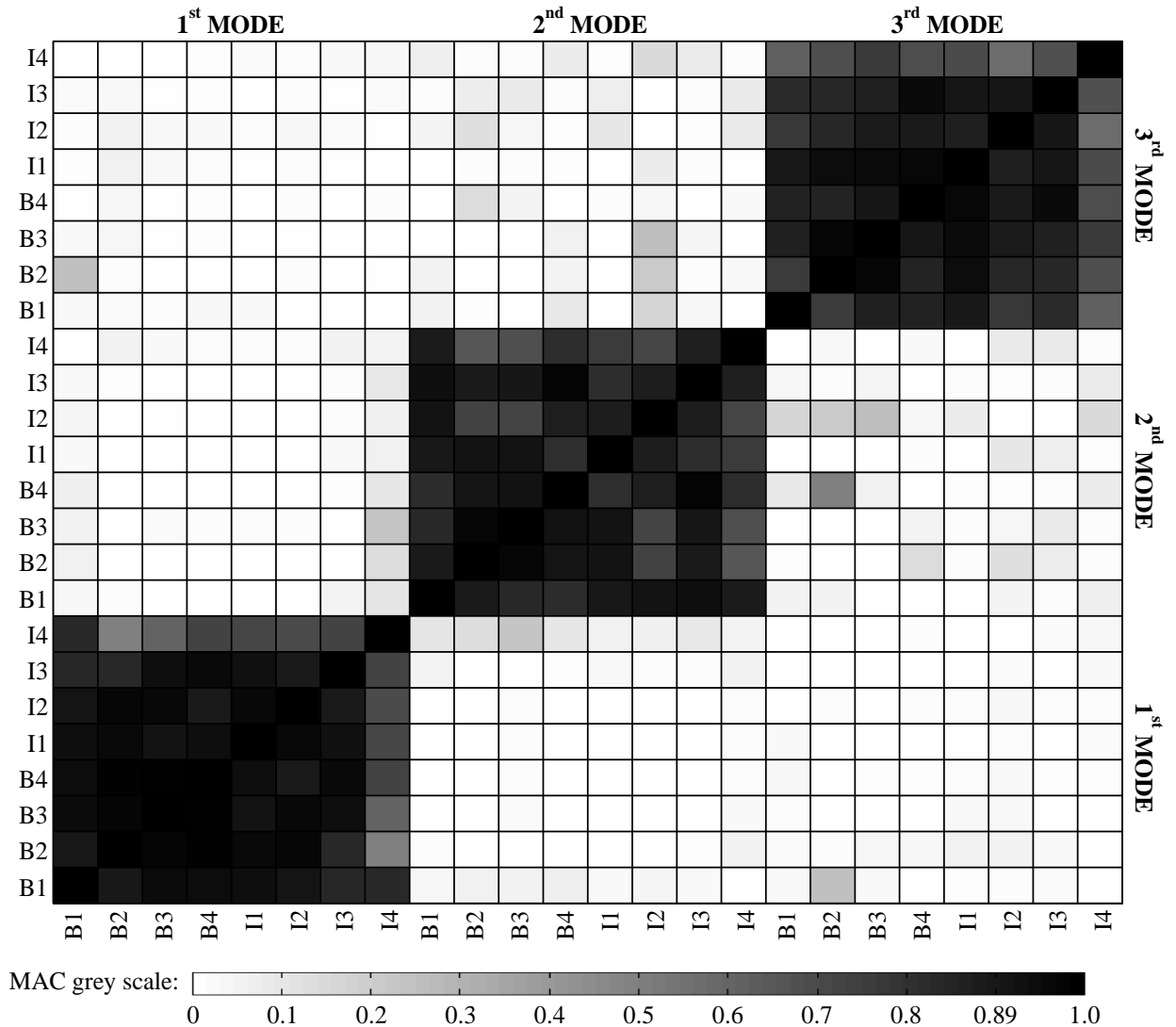


Figure 9. MAC values between the first three identified mode shapes for all construction phases.

Indeed, the almost white areas outside the diagonal, representing the comparison between the  $i$ -th mode shapes of a construction phase with all the  $j$ -th modes of the other phases, demonstrating that there are no changes in the typology of modes.

#### **4 Integration of ambient vibration tests with non-destructive in-situ tests**

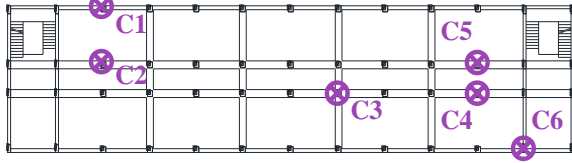
As already mentioned, the proposed monitoring methodology can take advantage of classical NDTs. For the case study at hand, UPTs and RHTs were performed; the former are used to assess the homogeneity and the mechanical and dynamic properties of concrete [38], while the latter are performed with the aims of assessing the overall concrete homogeneity for the whole building and of providing an estimation of the concrete compressive strength [39-40]. Furthermore, to reduce the uncertainties related to the concrete compressive strength estimation with the two above mentioned tests, the combined SONREB (SONic + REBound) [32] methodology is also adopted. Finally, during key stages of the construction process, further NDTs are performed, such as ILTs on selected infill masonry walls. These tests aim to identify the modal parameters that characterize the OOP dynamic behaviour of infills, through which an estimate of the infill mechanical properties and consequently of the infill IP stiffness can be obtained, according to the procedure proposed by Nicoletti et al. [24].

##### *4.1 Ultrasonic pulse tests on RC members*

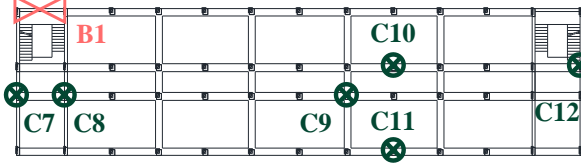
UPTs are performed on several RC structural elements: twenty-two Columns (C) and seven Beams (B) (identified in Figure 10a) located at different floors are investigated in order to include almost all the casting phases (seven of the nine casting phases are examined). All the tests are performed in the same day (September 30<sup>th</sup>, 2016) taking into account that the pulse propagation velocity, and consequently the concrete mechanical properties, are affected by temperature variations, humidity conditions and the age of concrete. Many tests for each RC member are performed to have a significant amount of data and to increase confidence with results, and the mean pulse velocity  $V_m$  is considered. Moreover, for some columns, tests are performed twice, varying the testing location, i.e. at mid-height and at the base, to investigate possible variations due to different concrete compacting conditions (Figure 10b). However, the latter were excluded by the test results. A summary of the results obtained at the end of the in-situ test campaign is reported in Table 5. For each casting phase, the number of the tested members is reported, together with the average casting phase pulse velocity  $\bar{V}_m$ , calculated as the average between the mean pulse velocities  $V_m$  of all members belonging to the same casting phase.

Based on the pulse velocity, several authors proposed correlation formulas with the compressive strength, although results of these tests are often only considered for a qualitatively estimation of the strength and of the concrete quality.

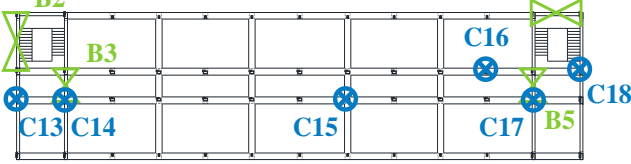
1<sup>st</sup> elevation columns and 1<sup>st</sup> floor



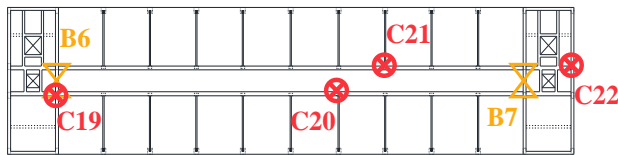
2<sup>nd</sup> elevation columns and 2<sup>nd</sup> floor



3<sup>rd</sup> elevation columns and 3<sup>rd</sup> floor

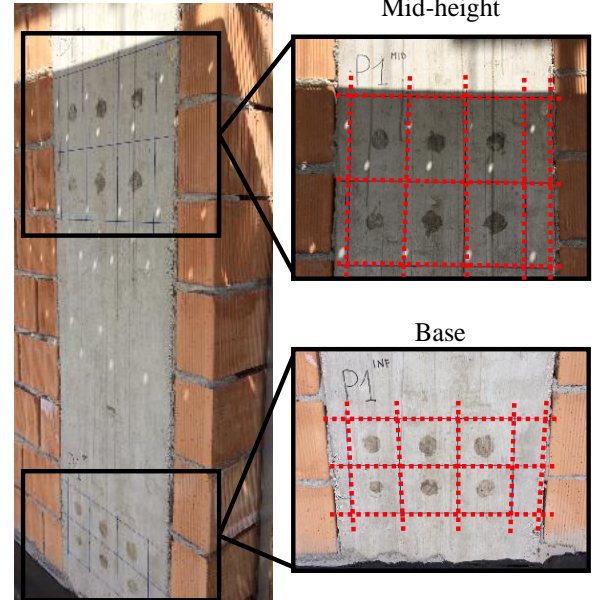
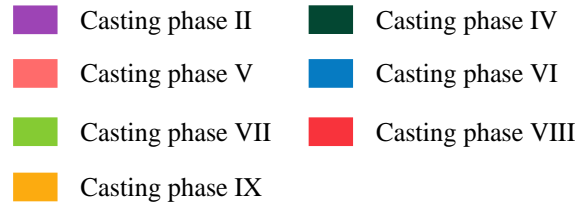


4<sup>th</sup> elevation columns and roof floor



(a)

Casting phase colour legend:



(b)

Figure 10. UPTs: (a) tests performed and investigated casting phases, (b) example of a test layout on a column.

Table 5. Summary of UPTs performed and average casting phase pulse velocities.

| Casting phase | Casting date (2016) | Description                          | N. of tested columns | N. of tested beams | $\bar{V}_m$ [m/s] |
|---------------|---------------------|--------------------------------------|----------------------|--------------------|-------------------|
| I             | May 20              | Foundation system and basement floor | ---                  | ---                | ---               |
| II            | May 27              | 1 <sup>st</sup> elevation columns    | 6                    | ---                | 4331              |
| III           | June 16             | 1 <sup>st</sup> floor                | ---                  | ---                | ---               |
| IV            | June 24             | 2 <sup>nd</sup> elevation columns    | 6                    | ---                | 4201              |
| V             | July 12             | 2 <sup>nd</sup> floor                | ---                  | 1                  | 4335              |
| VI            | July 19             | 3 <sup>rd</sup> elevation columns    | 6                    | ---                | 4283              |
| VII           | August 2            | 3 <sup>rd</sup> floor                | ---                  | 4                  | 4317              |
| VIII          | August 8            | 4 <sup>th</sup> elevation columns    | 4                    | ---                | 4284              |
| IX            | August 23           | Roof floor                           | ---                  | 2                  | 4209              |

Indeed, it is well known that a reliable correlation between UPT results and the relevant concrete compressive strength can be achieved only with the support of destructive compressive tests, performed on either in-situ members or through core or cubic samples. Among the others, two correlations can be considered: that of Leslie-Cheesman [41], which provides a qualitatively judgement of the concrete on the basis of the pulse velocity, and that of Whitehurst [42], which defines both a qualitatively judgment

and an estimation of the concrete compressive strength based on the pulse velocity. Based on the average casting phase pulse velocities  $\bar{V}_m$  of Table 5, the concrete is always classified as “good” according to [41], and “excellent” according to [42], with an estimated compressive strength around 40 MPa, greater than the design one ( $R_{ck} = 35$  MPa).

The pulse velocities can be adopted also to estimate the dynamic elastic modulus of concrete  $E_d$ , which characterizes the concrete behaviour for very low stress and strain levels, such as those produced by the ambient excitation. The dynamic elastic modulus can be estimated based on the wave propagation theory in homogeneous, isotropic, and elastic materials that provides the following expression:

$$E_d = \rho V^2 \frac{(1 + \nu_d)(1 - 2\nu_d)}{1 - \nu_d} \quad (1)$$

where  $\rho$  is the concrete mass density and  $\nu_d$  is the dynamic Poisson coefficient, assumed equal to 0.28, as suggested in [43]. The calculated dynamic elastic moduli  $E_d$  are reported in Table 6 for all casting phases; it emerges that values are very similar (ranging between 32.4 to 34.5 GPa) for all the casting phases, demonstrating an overall homogeneity of the concrete material for the whole building. Furthermore, dynamic elastic moduli are almost always greater than the static ones (Table 1), consistently with considerations reported in [43], that suggests values of the dynamic modulus 10-20% higher than the static ones. The previous consideration is not rigorously true for casting phases IV and IX, but differences are not so high to suggest construction defects. Moreover, the IX phase was poured on August 23<sup>rd</sup>, while the UPTs were developed on September 30<sup>th</sup>, so it is possible that the concrete maturation was not enough to respect suggestions derived in [43].

Table 6. Dynamic elastic moduli estimated for different casting phases.

| Casting phase | I   | II   | III | IV   | V    | VI   | VII  | VIII | IX   |
|---------------|-----|------|-----|------|------|------|------|------|------|
| $E_d$ [GPa]   | --- | 34.5 | --- | 32.4 | 34.5 | 33.7 | 34.2 | 33.6 | 32.6 |

#### 4.2 Rebound hammer tests on RC members

RHTs are performed on the same structural members tested with ultrasonic methodology; at least nine hammer impacts for each element surface are provided and the measured rebound numbers are recorded. Each RC element is tested twice, on two opposite surfaces; hence the rebound number that characterizes the element is calculated as the mean of the two rebound numbers of each face. Finally, the average rebound number  $\bar{N}_m$  of each casting phase is calculated, as the average between all rebound numbers of columns or beams belonging to the same casting phase. The results, listed in Table 7, show, as expected, higher values for the lower floors with respect to the higher ones, because of the different maturation periods. Anyway, differences between casting phases are not so high, proving that the concrete has similar mechanical properties on the overall structure.

An example of a generic relationship between the rebound number and the concrete grade (according to the classification proposed in [44]) is described in the Annex B of [40]. Based on this, it is possible to assert that the estimated concrete grade for the building is around C30/37 (only the rebound number of casting phase VIII theoretically leads to a lower concrete grade, but it constitutes a border line value with the higher grade), which is higher than the design concrete grade (C28/35). It is worth remembering that above considerations are merely qualitative, since a correlation with core or cubic sample compressive tests are needed to obtain information about the concrete compressive strength from rebound numbers. Anyway, RHTs can help the designers to control and validate the correctness of the construction procedures.

Table 7. Average rebound number for different casting phases.

| Casting phase | I   | II | III | IV | V  | VI | VII | VIII | IX |
|---------------|-----|----|-----|----|----|----|-----|------|----|
| $\bar{N}_m$   | --- | 45 | --- | 45 | 44 | 43 | 44  | 42   | 43 |

#### 4.3 Combination of ultrasonic pulse and rebound hammer test results: the SONREB methodology

To reduce uncertainties relevant to the concrete compressive strength estimation obtained with the previous test procedures, the combined SONREB [32] methodology is also adopted, merging information about the concrete surface strength (obtained from RHTs) and about the concrete quality throughout the cross section (obtained from UPTs). The SONREB methodology consists in estimating the concrete compressive strength  $R_c$  based on rebound numbers  $N$  and ultrasonic pulse velocities  $V$ , using an equation such as  $R_c = a N^b V^c$ , where  $a$ ,  $b$  and  $c$  are constants that can be derived through correlations between non-destructive and compressive test results. In this work, the coefficients are assumed equal to those provided in the literature and, more specifically, from [32]. Therefore, values of  $a = 1.2 \cdot 10^{-9}$ ,  $b = 1.058$  and  $c = 2.446$  are adopted.

The compressive strength  $R_c$  for each casting phase is estimated, adopting the mean casting phase pulse velocity  $\bar{V}_m$  (Table 5) and the mean rebound number  $\bar{N}_m$  (Table 7); the results are reported in Table 8. As can be noted, all values are between 47 and 52 MPa, proving that the in-situ concrete has a noticeably compressive strength, always greater than the design one.

Table 8. Estimated concrete compressive strength from SONREB methodology.

| Casting phase | I   | II | III | IV | V  | VI | VII | VIII | IX |
|---------------|-----|----|-----|----|----|----|-----|------|----|
| $R_c$ [MPa]   | --- | 52 | --- | 49 | 51 | 49 | 51  | 47   | 47 |

#### 4.4 Impact load tests on infill masonry walls

During key stages of the construction process ILTs are also performed on selected infill masonry walls. These tests aim to identify the modal parameters that characterize the OOP dynamic behaviour of

the infills, from which an estimation of the infill IP stiffness can be obtained adopting the procedure proposed by Nicoletti et al. [24]. In detail, the procedure allows estimating the Young's modulus of a homogeneous and isotropic material that can be used to model infills in Finite Element (FE) models adopting shell elements. The stiffness is representative of the IP and OOP behaviour of the infill subjected to low amplitude excitations, such as ambient actions. An instrumented hammer (PCB model 086D20) and two accelerometers (PCB model 353B43) are adopted to perform ILTs; for each tested wall, the two sensors are fixed on the panel in different positions, while impacts are provided in more than one point, with the aim of identifying as much vibration modes as possible, extending the identification also to superior modes. The impacts are provided in the direction orthogonal to the wall plane and accelerations are measured in the same direction. Input-output identification techniques can be adopted to identify the modal parameters of the panel, as suggested in [24].

Six masonry infills typologies, characterized by similar geometries and constructive features, can be identified in the building, as reported in Figure 2f. Among these, three walls, representative of the majority of the infill typologies, are selected to be experimentally investigated with ILTs (Figure 11). The selected walls are representative of all the internal infill typologies (W1 for I3, W2 for I1, W3 for I2); furthermore, assuming that the insulation layer on the exterior side of the external infill E3 does not influence its dynamic behaviour, it is reasonable to accept that E3 and I3 have nearly the same mechanical and material properties. Tested walls W1, W2 and W3, having thicknesses of 20, 8 and 12 cm, respectively, are represented in Figure 11. All walls, located at the underground level of the building, have similar dimensions (height and width), are confined by the RC frame, and have no openings. Walls are tested twice, before and after the plastering, in order to obtain stiffness properties that can be used in numerical models in all possible construction phases. The identified OOP vibration modes of each wall are reported in Table 9 with the relevant resonance frequency values, whereas Figure 12 depicts the corresponding mode shapes, obtained from data of tests after the infill plastering (mode shapes of infills without plaster present very similar mode shapes, sometimes less refined probably because of the most pronounced orthotropic behaviour, which is mitigated by the plaster layers). Each vibration mode is named with a couple of numbers ( $n,m$ ) that represent the number of semi-waves present in the mode shape along the horizontal and vertical directions, respectively. Many vibration modes are identified for each wall, especially for W2. Furthermore, being the dimensions of the three walls quite similar, the wall frequencies increase with the brick thickness, as expected. Additionally, the frequency values increase with the plastering, as predictable, presenting a mean percentage increase of about 36%, 35% and 48% for W1, W2 and W3, respectively.

The procedure proposed in [24] is adopted to obtain a reliable estimate of the infill stiffness, expressed in terms of elastic modulus of a homogenous isotropic material that can be adopted to define

the mechanical properties of the shell elements simulating the masonry infills in numerical models. The procedure leads to values ranging between 1500 and 3500 MPa for the walls without plaster, and to values between 3000 and 4500 MPa for the walls after the plastering. It is worth observing that these values agree with the typical elastic moduli proposed for infills with similar features, as reported in [45].

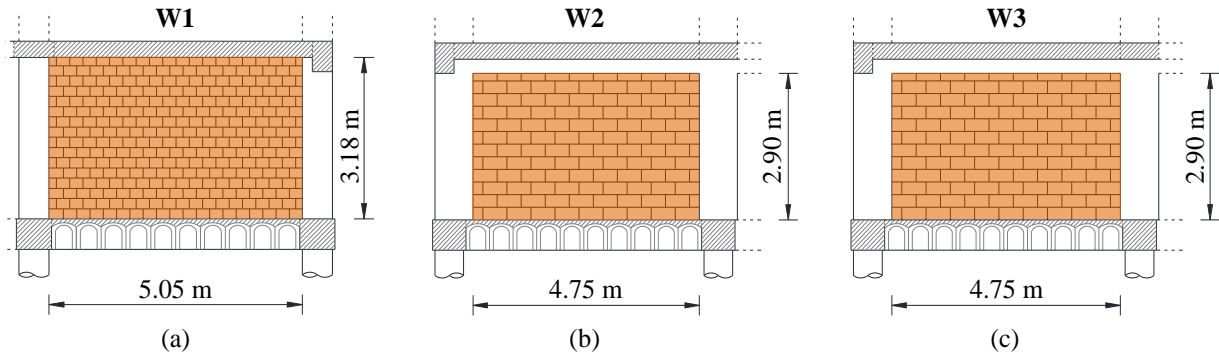


Figure 11. Tested wall geometries: (a) W1, (b) W2, (c) W3.

Table 9. Identified infill OOP vibration modes and relevant frequencies [Hz].

| W1   |                 |              | W2   |                 |              | W3   |                 |              |
|------|-----------------|--------------|------|-----------------|--------------|------|-----------------|--------------|
| Mode | without plaster | with plaster | Mode | without plaster | with plaster | Mode | without plaster | with plaster |
| 1,1  | 39.82           | 54.67        | 1,1  | 16.01           | 25.34        | 1,1  | 27.83           | 44.73        |
| 2,1  | 52.10           | 74.84        | 2,1  | 29.38           | 41.83        | 2,1  | 42.21           | 66.03        |
| 3,1  | 73.01           | 109.56       | 1,2  | 39.76           | 57.51        | 3,1  | 64.75           | 96.35        |
| 4,1  | 101.51          | 139.15       | 3,1  | 51.61           | 69.08        | 1,2  | 76.75           | 116.73       |
| 1,2  | 111.89          | 138.70       | 2,2  | 51.99           | 74.35        | 2,2  | 92.71           | 135.61       |
| 2,2  | 121.87          | 159.43       | 3,2  | 70.02           | 99.20        | 4,1  | 93.19           | 127.98       |
| 3,2  | ---             | 189.57       | 1,3  | 72.20           | 99.85        | 3,2  | 113.67          | 165.16       |
| 5,1  | 141.16          | 201.31       | 4,1  | 78.81           | 109.86       | 5,1  | 121.26          | 193.23       |
| 4,2  | 167.32          | 226.29       | 2,3  | ---             | 114.15       | 4,2  | 139.38          | 204.08       |
| 5,2  | 199.77          | 269.03       | 3,3  | 100.61          | 139.04       | 1,3  | 149.68          | 216.86       |
| 3,3  | ---             | 304.53       | 4,2  | 105.49          | 135.72       | 5,2  | 176.59          | 251.38       |
| 4,3  | 262.63          | 337.05       | 5,1  | 119.73          | 157.49       | 3,3  | 188.84          | 265.08       |
| 5,3  | 288.49          | 374.55       | 5,2  | 136.89          | 182.40       | 4,3  | ---             | 303.53       |
|      |                 |              | 4,3  | 163.95          | 171.50       | 5,3  | ---             | 347.93       |
|      |                 |              | 5,3  | ---             | 214.75       |      |                 |              |
|      |                 |              | 5,4  | ---             | 256.32       |      |                 |              |
|      |                 |              | 5,5  | ---             | 306.02       |      |                 |              |



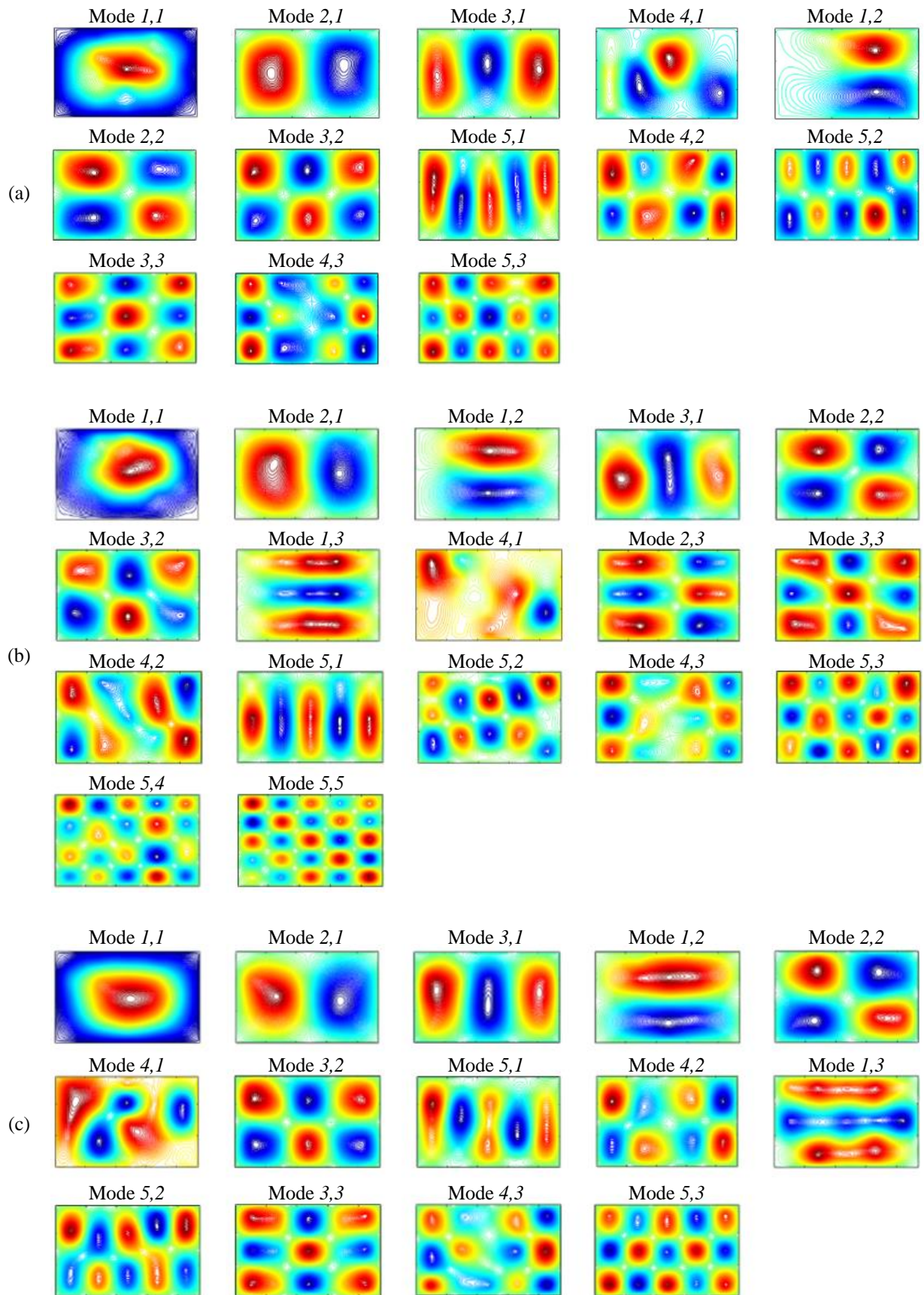


Figure 12. Mode shapes of the tested infill masonry walls (with plaster): (a) W1, (b) W2, (c) W3.

## 5 Comparison of time-frequency trends with numerical predictions

The evolution of the building experimental modal parameters during construction is compared with the expected numerical predictions, obtained through the support of a FE model of the building. The numerical model is developed within a commercial software for structural analysis [46], modelling beams and columns as frame elements, and floors and stair slabs as shell elements. The elevators are not modelled since they are disconnected from the building frame structure. For the sake of completeness, also the foundation system is considered, modelling piles and tie beams with frame elements. The soil-structure interaction is considered according to a Winkler approach adopting distributed independent springs, whose properties are obtained based on the soil properties and using well-known formulas available in the literature [47]. However, it is worth mentioning that also fixed base models have been investigated, obtaining slightly higher frequency values and almost equal mode shapes. Only the mass and loads effectively present on the structure at each construction stage are considered, neglecting consequently the live loads and some permanent loads, if not present yet. The concrete stiffness is assumed based on the dynamic elastic moduli obtained from NDTs since they better represent the concrete behaviour subjected to low excitation levels, as the ambient vibration. In detail, different dynamic elastic moduli are assigned to each casting phase, consistently with values obtained from UPT results. Finally, infill masonry walls are modelled with shell elements, considering their real positions, thicknesses, and openings. The infill mass is easily estimated on the basis of the construction materials adopted, which are known, whereas the stiffness is assumed on the basis of the elastic moduli estimated through ILTs on walls. For the wall typologies that are not tested (E1 and E2), a reasonable elastic modulus is estimated, based on tested wall results and elastic modulus values available in [45].

The building FE model has been updated step-by-step during the construction to represent as close as possible the real structure when the AVTs were performed (i.e. to represent the building in the eight monitoring phases). For the first four stages (bare structure), infills are removed, and only the constructed members are considered, removing those not built yet. The non-structural permanent loads are also neglected. The complete FE model of the bare structure, representing the construction phase B4, is illustrated in Figure 13a. For the last four stages the frame structure is not modified, while infills are added when they were built. Also, permanent non-structural loads are added, if present. A figure of the complete FE model, referring to the complete building (I4), is reported in Figure 13b.

Eigenvalues and eigenvectors of the models representative of all the construction phases are obtained through modal analyses exploiting the software potentials. In Table 10 the numerical natural frequencies (NUM) are compared with the experimental ones (EXP) discussed in Section 3. Furthermore, the numerical and experimental mode shapes are also compared in terms of MAC indexes. It can be observed that the numerical and experimental modal parameters show a very good agreement,

demonstrating a good consistency between the numerical design model and the real structure. The final numerical model, representing the phase I4, revealed able to capture very well the dynamics of the real building and can be used as a numerical tool to support interpretation of data from the SHM, and to investigate possible damage effects on the building, revealed by changes of modal properties.

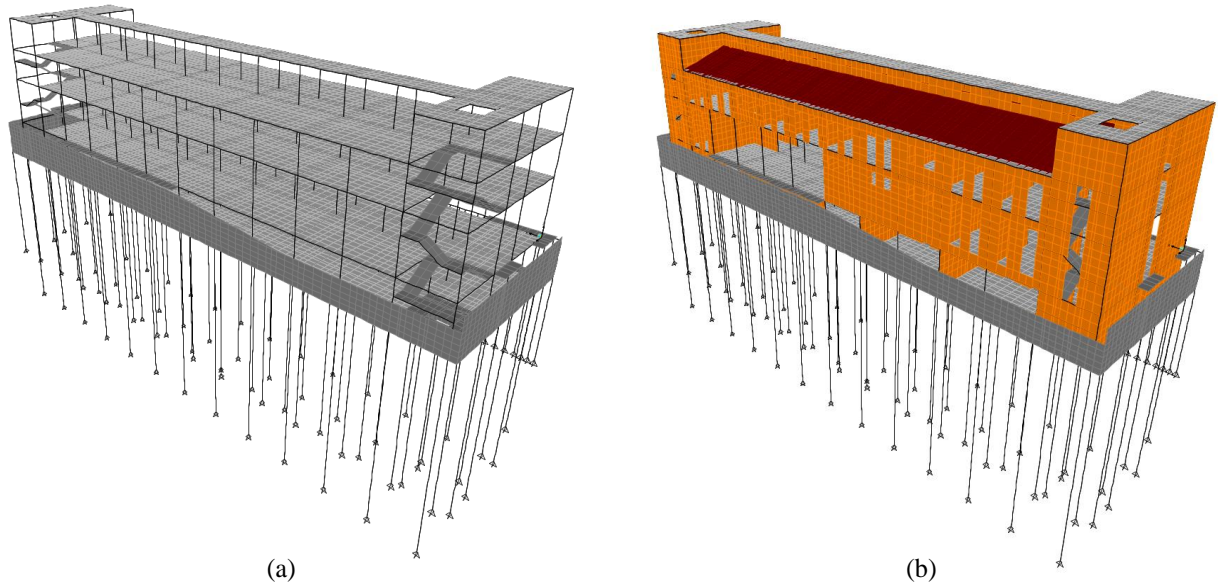


Figure 13. Building FE model: (a) complete bare frame (B4), (b) complete building (I4).

Table 10. Comparison between numerical and experimental modal parameters for all the monitored construction phases.

| Monitoring phase | 1 <sup>st</sup> vibration mode |      |      | 2 <sup>nd</sup> vibration mode |      |      | 3 <sup>rd</sup> vibration mode |      |      |
|------------------|--------------------------------|------|------|--------------------------------|------|------|--------------------------------|------|------|
|                  | Frequency [Hz]                 |      | MAC  | Frequency [Hz]                 |      | MAC  | Frequency [Hz]                 |      | MAC  |
|                  | NUM                            | EXP  |      | NUM                            | EXP  |      | NUM                            | EXP  |      |
| B1               | 4.55                           | 4.67 | 0.95 | 4.73                           | 4.95 | 0.90 | 5.44                           | 5.51 | 0.93 |
| B2               | 3.57                           | 3.47 | 0.97 | 4.32                           | 4.55 | 0.99 | 5.27                           | 5.18 | 0.94 |
| B3               | 2.87                           | 2.87 | 0.99 | 3.54                           | 3.66 | 0.99 | 4.50                           | 4.47 | 0.91 |
| B4               | 2.67                           | 2.62 | 0.98 | 3.35                           | 3.40 | 0.98 | 3.86                           | 4.19 | 0.93 |
| I1               | 4.00                           | 3.67 | 0.99 | 4.63                           | 4.47 | 0.91 | 5.04                           | 5.05 | 0.91 |
| I2               | 4.37                           | 4.36 | 0.99 | 4.96                           | 5.28 | 0.89 | 5.48                           | 5.63 | 0.83 |
| I3               | 5.50                           | 5.34 | 0.95 | 5.65                           | 5.89 | 0.98 | 6.43                           | 6.70 | 0.90 |
| I4               | 5.98                           | 6.02 | 0.90 | 6.07                           | 6.42 | 0.89 | 7.03                           | 7.06 | 0.81 |

## 6 Conclusions

In this paper a procedure to monitor RC buildings during construction is proposed. The procedure is based on the combination of conventional non-destructive tests and ambient vibration tests performed in key stages of the construction process, so as to create a sort of structural health monitoring during the construction. The procedure foresees the monitoring of the evolution of the building modal properties

during the main construction phases, through which an assessment of the correctness of the construction is possible through comparison with the expected trends. The following main benefits result from the application of the proposed monitoring strategy.

- Comparison of the real and numerical evolution of modal parameters makes it possible to verify in a simple and direct way if the building construction is correctly evolving, as well as to detect and investigate any possible anomalous trend; this procedure configures as a sort of proof testing during construction, which allow the overall building uncertainties to be reduced and the final certificate to be faster released.
- Tests on the bare frame can be suitably adopted to validate the design numerical model of the building, in which non-structural elements are usually neglected for verifications at ultimate limit states.
- The proposed monitoring allows the identification of the infills contribution on the building dynamics, providing useful information to address the interaction problem between structural and non-structural elements, which may reduce the global building ductility.
- Trends of resonance frequencies obtained from the monitoring during the construction, validated through comparisons with numerical data, can be suitably used as an important tool for the interpretation of data obtained from structural health monitoring systems.

A concluding remark is worth to be formulated with reference to the strategic constructions, for which also the integrity of non-structural components is an important issue in order to guarantee the building occupancy after exceptional events for the emergency management. Supposing the structure to be equipped with a structural health monitoring system, as is desirable for strategic buildings, the proposed strategy provides frequency thresholds relevant to different structural performances, including the absence of significant non-structural damage on the building. The latter can be adopted within a decision-making process to take proactive decisions in case of unexpected or anomalous behaviour due to ageing of material or seismic damage.

## References

- [1] Brownjohn J. M. W. Ambient vibration studies for system identification of tall buildings. *Earthquake Eng. Struct. Dyn.*, 32(1), 71-95, 2003.
- [2] Skolnik D., Lei Y., Yu E., Wallace J.W. Identification, model updating, and response prediction of an instrumented 15-story steel-frame building. *Earthquake Spectra*, 22(3), 781-802, 2006.
- [3] Zhang F. L., Ventura C. E., Xiong H. B., Lu W. S., Pan Y. X., Cao J. X. Evaluation of the dynamic characteristics of a super tall building using data from ambient vibration and shake table tests by a Bayesian approach. *Struct. Control Health Monit.*, 25(4), e2121, 2018.

- [4] Zhang J., Li Q. Identification of modal parameters of a 600-m-high skyscraper from field vibration tests. *Earthquake Eng. Struct. Dyn.*, 48(15), 1678-1698, 2019.
- [5] Ha T., Shin S. H., Kim H. Damping and natural period evaluation of tall RC buildings using full-scale data in Korea. *Applied Science*, 10(5), 1568, <https://doi.org/10.3390/app10051568>, 2020.
- [6] Al-Nimry H., Resheidat M., Al-Jamal M. Ambient vibration testing of low and medium rise infilled RC frame buildings in Jordan. *Soil Dyn. and Earthquake Eng.*, 59, 21-29, 2014.
- [7] Bindi D., Petrovic B., Karapetrou S., Manakou M., Boxberger T., Raptakis D., Pitilakis K. D., Parolai S. Seismic response of an 8-story RC-building from ambient vibration analysis. *Bull. Earthquake Eng.*, 13, 2095-2120, 2015.
- [8] Yousefianmoghadam S., Behmanesh I., Stavridis A., Moaveni B., Nozari A., Sacco A. System identification and modelling of a dynamically tested and gradually damaged 10-story reinforced concrete building. *Earthquake Eng. Struct. Dyn.*, 47(1), 25-47, 2018.
- [9] Ierimonti L., Venanzi I., Cavalagli N., Comodini F., Ubertini F. An innovative continuous Bayesian model updating method for base-isolated RC buildings using vibration monitoring data. *Mechanical Syst. and Signal Proc.*, 139, 106600, 2020.
- [10] Gara F., Carbonari S., Roia D., Balducci A. Seismic retrofit assessment of a school building through operational modal analysis and f.e. modelling. *J. of Struct. Eng.*, 147(1), 2021.
- [11] Kaplan O., Guney Y., Dogangun A. A period-height relationship for newly constructed mid-rise reinforced concrete buildings in Turkey. *Eng. Struct.*, 232(1), 2021.
- [12] Su R. K. L., Chandler A. M., Sheikh M. N., Lam N. T. K. Influence of non-structural components on lateral stiffness of tall buildings. *Struct. Design Tall Spec. Build.*, 14(2), 143-164, 2005.
- [13] Butt F., Omenzetter P. Seismic response trends evaluation and finite element model calibration of an instrumented RC building considering soil-structure interaction and non-structural components. *Eng. Struct.*, 65, 111-123, 2014.
- [14] De Angelis A., Pecce M. R. The structural identification of the infill walls contribution in the dynamic response of framed buildings. *Struct. Control Health Monit.*, 26(9), e2405, 2019.

- [15] Zhou Y., Pei Y., Hwang H. J., Yi W. Field measurements for calibration of simplified models of the stiffening effect of infill masonry walls in high-rise RC framed and shear-wall buildings. *Earthq. Eng. & Eng. Vib.*, 19, 87-104, 2020.
- [16] Gara F., Arezzo D., Nicoletti V., Carbonari S. Monitoring the modal properties of an RC school building during the 2016 Central Italy seismic swarm. *J. Struct. Eng. (ASCE)*, 147(7), 05021002, (2021).
- [17] Varum H., Furtado A., Rodrigues H., Dias-Oliveira J., Vila-Pouca N., Arede A. Seismic performance of the infill masonry walls and ambient vibration tests after the Ghorka 2015, Nepal earthquake. *Bull. Earthquake Eng.*, 15, 1185-1212, (2017).
- [18] Torkamani M. A. M., Ahmadi A. K. Stiffness identification of a tall building during construction period using ambient tests. *Earthquake Eng. Struct. Dyn.*, 16(8), 1177-1188, 1988.
- [19] Ventura C. E., Schuster N. D. Structural dynamic properties of a reinforced concrete high-rise building during construction. *Canadian J. Civil Eng.*, 23(4), 950-972, 2011.
- [20] Nunez T. R., Boroshek R. L., Larrain A. Validation of a construction process using a structural health monitoring network. *J. Performance and Constr. Facilities.*, 27(3), 270-282, 2013.
- [21] Astroza R., Ebrahimian H., Conte J.P., Restrepo J.I., Hutchinson T.C. Influence of the construction process and nonstructural components on the modal properties of a five-story building. *Earthquake Eng. Struct. Dyn.*, 45(7), 1063-1084, 2016.
- [22] Wang X., Hutchinson T. C. Evolution of modal characteristics of a mid-rise cold-formed steel building during construction and earthquake testing. *Earthquake Eng. Struct. Dyn.*, 49(14), 1539-1558, 2020.
- [23] Moaveni B., He X., Conte J. P., Restrepo J. I., Panagiotou M. System identification study of a 7-story full-scale building slice tested on the UCSD-NEES shake table. *J. Struct. Eng.*, 137(6), 2011.
- [24] Nicoletti V., Arezzo D., Carbonari S., Gara F. Expeditious methodology for the estimation of infill masonry wall stiffness through in-situ dynamic tests. *Constr. Build. Mat.*, 262, 120807, 2020.

- [25] De Angelis A., Pecce M. R. The structural identification of the infill walls contribution in the dynamic response of framed buildings. *Structural Control and Health Monitoring*, 26:e2405, 2019.
- [26] Di Trapani F., Shing P. B., Cavaleri L. Macroelement model for in-plane and out-of-plane responses of masonry infills in frame structures. *Journal of Structural Engineering (ASCE)*, 144(2), 04017198, 2018.
- [27] Perrone D., Leone M., Aiello M. A. Non-linear behaviour of masonry infilled RC frames: Influence of masonry mechanical properties. *Engineering Structures*, 150, 875-891, 2017.
- [28] Zhou Y., Zhou Y., Yi W., Chen T., Tan D., Mi S. Operational modal analysis and rational finite-element model selection for ten high-rise buildings based on on-site ambient vibration measurements. *J. Perform. Constr. Facil.*, 31(5), 04017043, 2017.
- [29] Regni M., Arezzo D., Carbonari S., Gara F., Zonta D. Effect of environmental conditions on the modal response of a 10-story reinforced concrete tower. *Shock and Vibration*, 9476146, 2018.
- [30] Ubertini F., Gentile C., Materazzi A. L. Automated modal identification in operational conditions and its application to bridges. *Engineering Structures*, 46, 264-278, 2013.
- [31] Rainieri C., Magalhaes F., Gargaro D., Fabbrocino G., Cunha A. Predicting the variability of natural frequencies and its causes by second-order blind identification. *Structural Health Monitoring*, 18(2), 486-507, 2019.
- [32] RILEM. NDT 4 Recommendations for in-situ concrete strength determination by combined non-destructive methods. *Compendium of RILEM Technical Recommendations*, E&FN Spon, London, 1993.
- [33] Ewins D. J. *Modal testing: Theory, Practice and Application*. Research studies press ltd, Baldock, Hertfordshire, England.
- [34] Van Overschee P., De Moor B. *Subspace identification for linear systems: theory–implementation–applications*. Dordrecht, The Netherlands: Kluwer Academic Publishers, 1996.
- [35] Tian M. G., Yi W. J. Dynamic behaviour of reinforced concrete frame structure during construction. *J. Cent. South Univ. Technol.* 15, 418-422, 2008.



- [36] Carbonari S., Morici M., Dezi F., Leoni G. A lumped parameter model for the time-domain inertial soil-structure interaction analysis of structures on pile foundations. *Earthq. Eng. Struct. Dyn.*, 47(11), 2147-2171, 2018.
- [37] Allemang R. J., Brown D. L. A correlation coefficient for modal vector analysis. *Proc. of 1<sup>st</sup> Int. Modal Analysis Conf.*, Bethel, CT, USA, 110–15, 1982.
- [38] European Committee for Standardization (CEN). Testing concrete in structures – Part 4: Non-destructive testing - Determination of ultrasonic pulse velocity. EN 12504-4:2004.
- [39] European Committee for Standardization (CEN). Testing concrete in structures – Part 2: Non-destructive testing - Determination of rebound number. EN 12504-2:2012.
- [40] European Committee for Standardization (CEN). Assessment of in-situ compressive strength in structures and precast concrete components. EN 13791:2019.
- [41] Leslie J. R., Cheesman W. J. An ultrasonic method for studying deterioration and cracking in concrete structures. *J. of American Concrete Institute*, 21(1), 17-35, 1949.
- [42] Whitehurst E. A. Soniscope tests concrete structures. *ACI Journal Proceedings*, 47(6), 433, 1957.
- [43] Popovics J. S., Zemajtis J., Shkolnik I. ACI-CRC Final Report – A study of static and dynamic modulus of elasticity of concrete. American Concrete Institute, 2008.
- [44] European Committee for Standardization (CEN). Design of concrete structures – Part 1-1: General rules and rules for buildings. EN 1992-1-1:2015.
- [45] Frumento S., Magenes G., Morandi P., Calvi G. M. Interpretation of experimental shear tests on clay brick masonry walls and evaluation of q-factors for seismic design. Research report EUCENTRE 2009/02, EUCENTRE and University of Pavia, Pavia, 2009.
- [46] SAP2000 advanced (v23.0) Static and dynamic finite element analysis of structures, Berkeley, CSI Computer & Structures, Inc., 2021.
- [47] Gazetas G., Makris N. Dynamic pile-soil-pile interaction. Part I: Analysis of axial vibration. *Earthquake Engineering & Structural Dynamics*, 20(2), 115-132, 1991.